Deep Structure, Singularities, and Computer Vision

DSSCV

IST-2001-35443

Deliverable

Deliverable No. 4	4
Title:	Symmetry Sets and Medial Axes in Two Dimensions
Author(s):	Peter Giblin and André Diatta
Institution:	University of Liverpool
Classification:	Public
Date:	21 March 2003

Abstract

We give a summary of the known results about the local geometry of the medial axis (MA) and the symmetry set (SS) of a curve in the plane, and how they evolve through a 1-family of curves. We discuss in

more detail a begining of investigations in the case of evolutions of the SS/MA in families of curves obtained as sections of a surface, and about the the flow of the radius function of SS/MA. This is work in progress.

1 The local structure of symmetry sets and medial axes in 2D.

In this section, we wish to describe the local geometry of the SS/MA near its singularities. The classification in dimensions 2 and 3 is in [5].

Definition 1.0.1. *The symmetry set (SS, for short) of a closed curve $\mathcal{C}$ in $\mathbb{R}^2$ is the closure of the locus of centres of circles that are tangent to $\mathcal{C}$ at two points (bitangent circles), at least. The medial axis (MA) is the set of centres of circles bitangent to the curve and completely inside or completely outside $\mathcal{C}$. The levels bifurcation set of a family of functions $f(t,x)$ of variables t with parameters x is the union of the set of points where the function f with x fixed has two different singular points x, y having the same image $f(x) = f(y)$, and the set of degenerate singular points, ie the singularities where the second derivative of f with respect to t is degenerate.*

Notation. We use the standard A_k notation of Arnol'd, so that A_1 means ordinary tangency between a curve and a circle, A_2 means 3-point contact, A_3 means 4-point contact, and so on. We also write A_kA_n for a single circle having contacts with our curve of type A_k, A_n at distinct points, and abbreviate A_1A_1 to A_1^2, etc.

Let $\gamma : I \to \mathbb{R}$ be a closed smooth curve and set $\mathcal{C} = \gamma(I)$. Consider the associated family of distance-squared functions $F_\gamma : \mathcal{C} \times \mathbb{R}^2 \to \mathbb{R}$, $F_\gamma(t,v) = ||\gamma(t) - v||^2$. The evolute and the SS of $\mathcal{C}$ together make up the levels bifurcation set of F_γ. This is the way in which singularity theory can help with the description of symmetry sets.

1.1 Counting conditions: the number of types of singularities.

We give here a heuristic argument which limits the possible singularities which we need to consider. Formally, we can show that, for an open dense set of simple closed plane curves, only the given singularities will occur. Some analogous transversality calculations are given in [4, Ch.9].

At an informal level, transversality results such as this boil down into a compatibility between the number of equations defining the singularities of extended distance-squared function and the number of variables—that is, counting conditions. Namely, in $\mathbb{R}^2$ for singularities of type

• A_1^k: there are k variables defining the k points A_1 and 3 other variables for the coordinates (a,b) and the radius r of the circle. On the other hand, there are $2k$ conditions for both the intersection and the tangency of the circle and $\mathcal{C}$ at those k A_1-points. Hence, one must have $2k \leq k+3$. That is, only A_1, A_1^2 or A_1^3 can occur.

• $A_1^kA_2^p$: using the same argument as above, we must have $2k$ conditions for A_1^k, $2p$ conditions for A_2^p and p other conditions for the second derivatives of F_γ at the p points of type A_2, while the number of variables is k for A_1^k, p for A_2^p and 3 for the centre and the radius of the circle. Altogether, one should have $2k + 3p \leq k + p + 3$, that is $k = p = 1$ and we have only A_1A_2.

In this way, we deduce that for generic curves in the plane, the associated distance-squared function has only A_3, A_1A_2, A_1^3, A_2, A_1^2 and A_1 points as possible generic singularities. Note that A_1 by itself does not contribute to the SS (nor to the evolute nor the full bifurcation set of F).

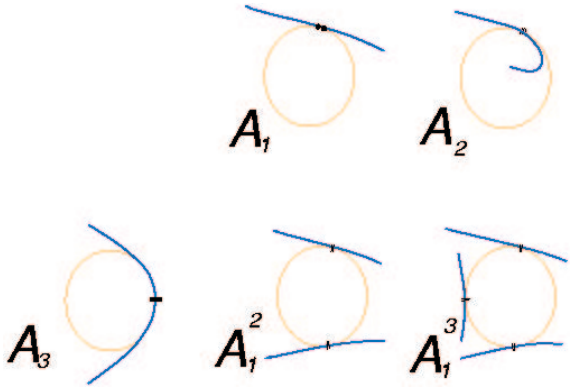

Figure 1: Illustration of the A_1, A_2, A_3, A_1^2, A_1^3 and A_1A_2 tangency with circles.

1.2 Behaviour of SS near the singularities.

Now we need to check the behaviour of the SS/MA in each individual case. This is done by using the uniqueness of versal, and multi-versal, unfoldings. That is, one checks that, for each of the singularities mentioned above, the family F_γ is (multi)versally unfolded by the variables $v = (x, y)$. From the uniqueness result of the local structure of the bifurcation set of multi versal unfoldings of a given singularity, the bifurcation set of F_γ is locally the same as that one of the normal form for that singularity. We can look for a local normal form of unfoldings of F_γ at each singularity and then derive the behaviour of its symmetry set near such a singularity.

A list normal forms at the above singularities is provided by standard techniques in singularity theory.

The symmetry set and the evolute have one of the four following normal forms **[5]**, the first two of which are rather trivial. All of these are illustrated in the next section, where we consider families of curves.

$\mathbf{A_2}$: If $f : t \mapsto f(t) = F_\gamma(t, x_o, y_o) = ||\gamma(t) - (x_o, y_o)||^2$ has an A_2 singularity at $t = 0$, then F_γ is always a versal unfolding of f and has standard normal formal $G(t, a, b) = t^3 + at$. It follows that the full bifurcation (=evolute + SS) set of any curve γ close to A_2 singularities is locally diffeomorphic to that of any versal unfolding with two parametres of an A_2 singularity. In this case the symmetry set has no component close to an A_2 singularity: there are no values of x_o, y_o allowing two singularities at the same level. Thus A_2 gives only the local structure of the evolute.

The FBS of the standard form G is $FBS_G = \{(a, b)|\exists t_o, \frac{dG}{dt}(t_o, a, b) = 0$ and $\frac{d^2G}{dt^2}(t_o, a, b) = 0\} = \{(a, b)/\exists t_o, 3t_o^2 + a = 0$ and $6t_o = 0\} = \{(0, b), b \in \mathbb{R}\}$. That is, the evolute is locally smooth.

$\mathbf{A_1^2}$: it is the centre of a (bitangent) circle which has ordinary contact with the curve at two differents places. An A_1^2 is an ordinary smooth point of the SS (and the MA when appropriate). This time there are no degenerate singularities close to the A_1^2. The standard 2-parameter multi-versal unfolding in this case is
$G_1(t_1, a, b) = \pm t_1^2$
$G_2(t_2, a, b) = \pm t_2^2 + a$

We just have $FBS_G = \{(a, b), a = 0\}$ which is locally smooth.

$\mathbf{A_1A_2}$: the centre of a bitangent circle which is the (osculating) circle of curvature at the (A_2-)tangency point on the curve, the other tangency point being an ordinary point contact. This means that the circle

crosses the curve at that point, so it is not a maximal circle. The A_1A_2 point is not in the MA and—see below—is a smooth point on the evolute and an ordinary cusp on the SS.
The standard multi-versal unfolding is
$G_1(t_1, a, b) = t_1^3 + at_1 + b$,
$G_2(t_2, a, b) = \pm t_2^2$.

FBS= $\{(a, b), \exists t_1$ such that $3t_1^2 + a = 0$ and $6t_1 = 0\} \cup \{(a, b), \exists t_1, t_2$ such that $3t_1^2 + a = 0, 6t_2 = 0$ and $t_1^3 + at_1 + b = t_2^2\}$ = b-axis $\cup \{(a = -3t_1^2, b = 2t_1^3)\}$. The first of these is the local evolute (smooth) and the second is the symmetry set (cusp).

$\mathbf{A_1^3}$: the centre of a circle (ordinary) tangent to the curve at three different places. It is a triple crossing on the SS and, if appropriate, the MA.
The standard multi-versal unfolding is
$G_1(t_1, a, b) = \pm t_1^2$
$G_2(t_2, a, b) = \pm t_2^2 + a$
$G_3(t_3, a, b) = \pm t_3^2 + b$.
In this case the full bifurcation set has no component of degerate singularities but has three components $a = 0,\ b = 0,\ a = b$, that is three transversal smooth branches.

$\mathbf{A_3}$: this is the centre of a circle of curvature at a vertex on the (A_3-)contact point with the curve. An A_3 point is on the MA when the curvature is a maximum (or a negative maximum), but not a minimum (or a negative minimum). It is an endpoint of the SS or MA, in a cusp of the evolute. The standard versal unfolding (just one point is in question here) is:
$G(t, a, b) = \pm t^4 + at^2 + bt$
FBS= $\{(a, b), \exists t$ such that $4t^3 + 2at + b = 0$ and $12t + 2a = 0\} \cup \{(a, b), \exists t_1, t_2$ such that $t_1^4 + at_1^2 + bt_1 = t_2^4 + at_2^2 + bt_2$ and $4t_1^3 + 2at_1 + b = 0\ 4t_2^3 + 2at_2^1 + b = 0\} = \{(a, b) = (-6t^2, -2t^3)\} \cup$ $\{$ half line $a < 0\}$.

2 The evolution of SS/MA in generic families.

We summarise here, the main results of the study of the following problem: what happens to the SS/MA as the curve evolves under in a generic 1-parameter family? The list of all non equivalent (up to a local diffeomorphism) evolutions is provided by J.W. Bruce & P.J. Giblin in **[3]** for the SS and by I.A.Bogaevsky and P.J. Giblin & B. Kimia **[1, 13]** for the MA.

The techniques are almost the same as above, except that we have an extra variable, the parameter in the family of curves. The existence of such an additional variable means that we now need to unfold our distance-squared function by three variables, instead of two as before. However, a major difference in the present case is that the full bifurcation set, which represents all the symmetry sets (and evolutes) of the whole family of curves, must be 'sliced' in order to recover the individual symmetry sets. This amount to taking sections by the level sets of a generic function. A good deal is known about generic functions on bifurcation sets (and their close relations, discriminants), many of the results being due to J.W.Bruce; see e.g. [2].

2.1 The General case

First of all, let $\gamma_t : I \to \mathbb{R}^2$, $\gamma_t(s) = (\gamma_1(s, t), \gamma_2(s, t))$ be a family of smooth curves: here t is the parameter in the family and s is the parameter on each curve. Consider the 'big family' of distance-squared functions $F_\gamma : I \times \mathbb{R} \times \mathbb{R}^2 \to \mathbb{R}$, $(s, t, v) \to ||\gamma_t(s) - v||^2 = (\gamma_1(s, t) - v_1)^2 + (\gamma_1(s, t) - v_2)^2$.

F is regarded as a 3-parameter unfolding of the distance-squared function $f(s) := F_\gamma(s, 0, v_o)$ from $v_o = (x_o, y_o)$. In the 'counting conditions' we will now have one more variable, so that, new types of singularities that were not allowed in the previous case of a single curve, namely $A_1^4,\ A_1A_3,\ A_2^2,\ A_1^2A_2,\ A_4$ types now appear, in addition to what we already have for a single curve. Here again, the distance squared function versally unfolds all its singularites of all types, that appear. (In the present case there is a condition on the genericity of the family itself as well as a requirement that the singularities are of exactly the types stated.)

Again the uniqueness of the full bifurcation set (FBS) of versal unfoldings implies that the (standard) FBS of the canonical form G, in say (a, b, c)- space, is locally diffeomorphic to the full FBS of the geometrical example at hand, that is the union of the symmetry sets and evolutes of the curves of the family under consideration.

So, the method can be summarized as follows. Given a singularity of the family F of distance-squared functions on a 1-parameter family of curves

• write its canonical form G; as in the single curve case, this will have one formula corresponding to each separate singularity, for example $A_1^2A_2$ will have three formulae,

• work out the bifurcation set of G,

• classify all possible ways of slicing the FBS of G using sections, near the singularity by using generic functions on the FBS.

• finally, having sufficient information about the isomorphism $F \simeq G$ one can decide whether any particular family of SS is possible.

The last point here is very significant: the total list of 'evolutions of the full bifurcation set' contains many situations which simply cannot arise geometrically in the context of families of curves. The full bifurcation set is present in many other contexts, for example in the study of height functions on surfaces, which amounts to the study of contact between surfaces and planes, and the evolution of parabolic curves on surfaces. In this context *all* the possible evolutions of FBSs occur. See [6, p.301].

We present here some examples; schematic pictures of these transitions are in Figure 2 and three of them are illustrated in the actual examples of Figures 3,4,**??**, which come from [8].

Here is a summary of the transitions which can occur. Some further details of these are in Section 4 on the behaviour of the radius function in a family of curves.

– The A_1^4 case. It corresponds to the centre of a circle tangent to the curve at four distinct A_1-points, of ordinary tangency.

– A_1A_3. A new structure immediately appears on the MA. This happens when a circle of curvature at a vertex of the boundary curve is tangent to this curve elsewhere. A formerly invisible branch of MA (i.e. a branch which is on the SS but not on the MA) with an endpoint becomes visible (part of the MA) as it penetrates an existing smooth branch of the MA, emerging as a part of a triple junction of MA branches. See Figure 3. This can also be an interaction simply between two branches of the SS, both of which may be 'invisible' (not on the MA) before and after the transition.

– $A_1^2A_2$. This is the centre of an osculating circle which has (ordinary) tangency with the curve at two other points.

– A_2^2. centre of a biosculating circle, that momentarily appears during the changes. Such a circle is not maximal as it has to cross the curve and an A_2^2-singularity of F_γ is never in the MA.

There are two ways in which an A_2^2 singularity can appear during the evolution.
In the so-called 'nib' transition, two cusps on the symmetry set interact and 'exchange branches'. Before the interaction, for branches appear in some order, say 1 and 2 paired, 3 and 4 paired. Now after the A_2^2 transition, the new pairs are $(1, 3)$ and $(2, 4)$ (see Figures 4,2).

In the 'moth' case, there are no endpoints in the SS, but four cusps are created.

- A_4 This occurs when the curve acquires a‘degenerate vertex’, which is the moment of birth (or death) of two ordinary vertices, one a maximun and the other a minimum of curvature. This is never visible on the MA, since a circle with an A_4 contact has five coincident contact point with the curve and therefore (5 being odd) must cross the curve. See Figure 3.

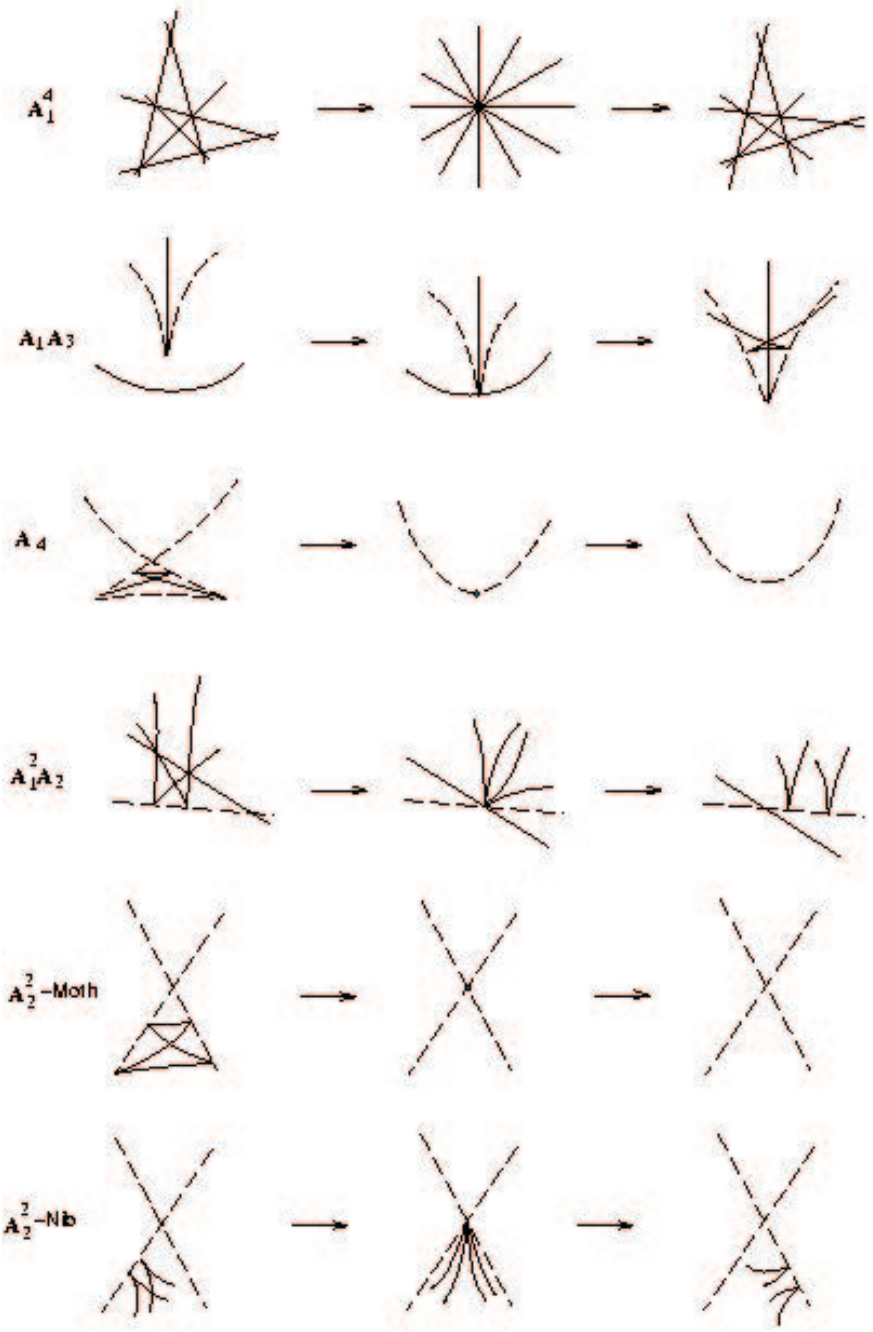

Figure 2: All ss-transitions in 1-parameter family of curves

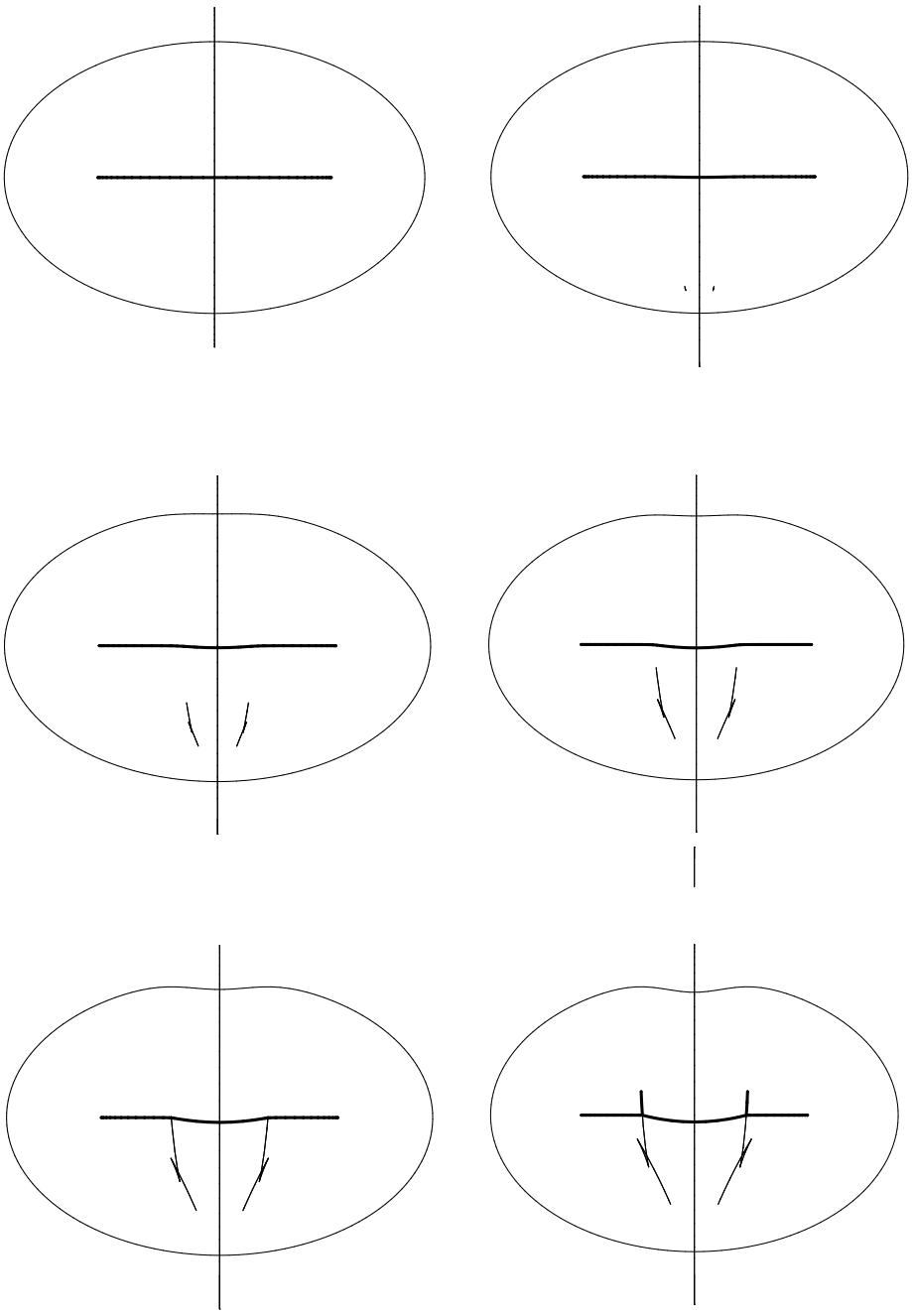

Figure 3: Illustration of an A_4 transition (a new branch of the SS) and an $A_1 A_3$ transition (piercing of a branch by another branch).

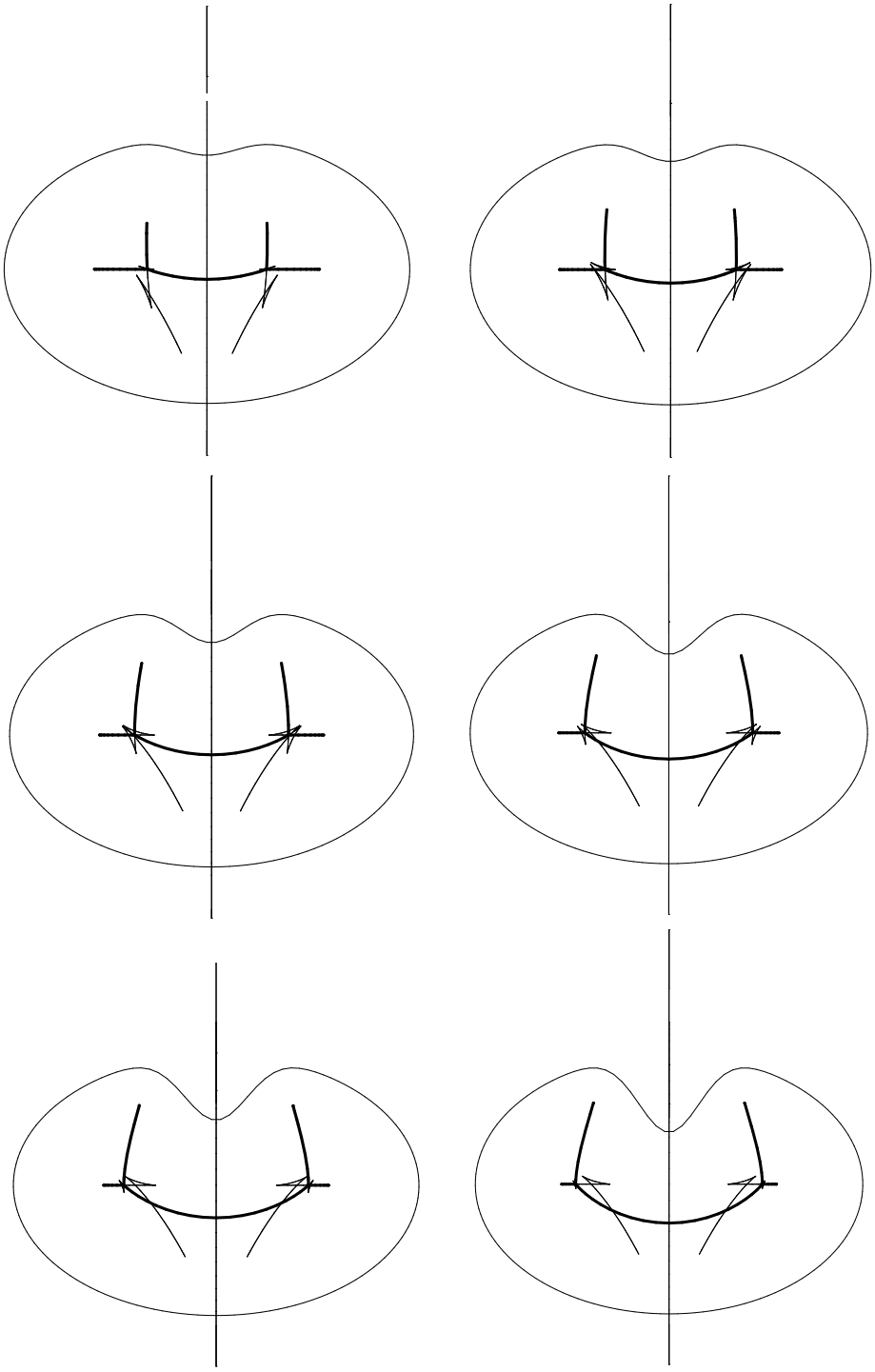

Figure 4: Illustration of an A_2^2 (nib) transition on SS.

2.2 1-parameter families determined by scale

Recall that 1-parameter families of curves determined by scale and passing through $\tilde{\gamma}(s,0) = \gamma(s)$ are obtained by Gaussian blurring and are solutions of the heat equation (see e.g. Teixeira **[15]**). Let us first show the connection between the heat equation and the curvature motion. Then we will state Teixeira's results concerning the particular case where the curve undergoes a 1-parameter family determined by scale. Denote $\Delta\gamma = (\Delta\gamma_1, \Delta\gamma_2)$ for a curve $\gamma := (\gamma_1, \gamma_2)$. Clearly, a solution $\tilde{\gamma}(s,t)$ of the (geometric) heat equation $\frac{\partial\tilde{\gamma}(s,t)}{\partial t} = \Delta\tilde{\gamma}$ satisfies the 'mean curvature motion (MCM)' equation $\frac{\partial\tilde{\gamma}(s,t)}{\partial t} = \frac{\partial^2\tilde{\gamma}}{\partial s^2} = \frac{\partial\mathbf{T}}{\partial s} = \kappa\mathbf{N}$. On the other hand, it is easy to establish that a family of curves evolving through MCM is a solution of the geometric heat equation.

Let s be here arclengh on the curve $\tilde{\gamma}$, so that the tangent vector $\mathbf{T} := \frac{\partial\tilde{\gamma}}{\partial s}$ is unit. The expression $\kappa\mathbf{N} = \frac{\partial\mathbf{T}}{\partial s} = \frac{\partial^2\tilde{\gamma}}{\partial s^2} = \Delta\tilde{\gamma}$ leads to the heat equation, as $\kappa\mathbf{N} = \frac{\partial\tilde{\gamma}}{\partial t}$ by definition of the MCM. That is $\frac{\partial\tilde{\gamma}}{\partial t} = \Delta\tilde{\gamma}$.

Notice that the above relations only hold for an infinitesimal step of t, since arclengh in not preserved by time t. Indeed, in this case, the variation of arclengh is not constant in general and

$$\frac{\partial}{\partial s}(\frac{\partial s}{\partial t}) = \kappa^2 \tag{1}$$

More precisely, we have

$$\frac{\partial}{\partial t}\frac{\partial}{\partial s} - \frac{\partial}{\partial s}\frac{\partial}{\partial t} = \kappa^2\frac{\partial}{\partial s} \tag{2}$$

as can be seen in **[10]** for example.

For the purpose of discovering the infinitesimal changes in the SS or MA during motion under the heat equation, it is therefore enough to use MCM.

Now let us discuss about what symmetry sets do occur in the case of Mean Curvature Motion (MCM). For the type of singularities of the distance squared function F_γ, the vanishing conditions on the derivatives of F_γ involve the curvature and its derivatives. In the case of MCM, those conditions imposes that symmetry sets allowed are the following **[15]**.

• The medial axis ('swallowtail') in the A_4 case: the direction of transition always causes the additional component of the SS to vanish.

• The 'swallowtail with half line' case in the A_1A_3 singularity: both directions of transitions can occur.

• The 'moth' and 'nib' in the A_2^2 case: the directions they go depend on κ and its derivatives, but the conditions for the two scenarios (a moth shrinking to a point a disappearing, and two interlaced cusps touching and separating) are always satisfied.

• The cusps in the $A_1^2A_2$: either directions are allowed.

• The A_1^4 symmetry set transition (quadrilateral flip): both directions of changes are equally allowed (indeed they are indistinguishable).

2.3 Symmetry sets of families of curves obtained by taking parallel sections of a surface.

In this section, we shall begin an investigation of the changes which occur in the medial axis and the symmetry set for a family of sections of a surface in $\mathbf{R^3}$. At the present time we have investigated examples, which appear to us to illustrate two of the important transitions. In both cases, the transition of the medial axis appears to be straightforward, but that of the symmetry set appears to be complex and in fact discontinuous. It is not clear at present how to approach these changes through a general application of singularity theory.

We think of our surface M as locally given by $z = f(x, y)$ for some smooth function f, the family of sections being given by varying z. We shall therefore consider the family of plane curves $f(x, y) = c$ as c varies. The only case which is not covered by the general evolution of symmetry sets of families of curves is when the tangent plane to M is the x, y plane at the origin of x, y, z-space. In all other cases the family of curves remains nonsingular as c passes through the value 0, and the general theory (Section 2) applies. There is clearly a major difference when the section $f(x, y) = 0$ is singular. There are four generic cases to consider:

Case 1. M has an elliptic point at the origin, so that $f(x, y) = 0$ is a single point locally.
Case 2. M has a hyperbolic point at the origin, so that $f(x, y) = 0$ is a pair of smooth intersecting curves locally.
Case 3. M has a parabolic point at the origin, so that $f(x, y) = 0$ is a curve with an ordinary cusp.
Case 4. M has a cusp of Gauss at the origin.

In Cases 1 and 2 the tangent plane has A_1 contact with M at the origin; in Case 3 the contact is A_2 and in Case 4 the contact is A_3.

Case 1 appears to be relatively straightforward: we expect the section of the surface to be 'like an ellipse' for small values of c, so that one branch of the medial axis gets shorter and disappears as c changes so that the plane moves off the surface, and likewise one branch of the symmetry set also disappears. In this report we shall examine examples of Cases 2 and 3 in some detail. This is ongoing work, and further results will be reported at a later stage.

Hyperbolic point at the origin We take as our model of this the sections of a torus in 3-space, by a family of planes parallel to the axis of the torus (where the latter is regarded as a surface of revolution about this axis). This produces a family of curves which passes through a 'saddle' transition. Here is the setup. We take the torus obtained by rotating the circle $\{(a + b\cos\theta, 0, b\sin\theta)\}$ about the z-axis in (x, y, z)-space. Thus the torus is parametrized by

$$x = (a + b\cos\theta)\cos\phi, \quad y = (a + b\cos\theta)\sin\phi, \quad z = b\sin\theta,$$

where $0 \leq \theta \leq 2\pi$, $0 \leq \phi \leq 2\pi$. We assume $a > b > 0$. Now we want to consider sections $x =$constant, say $x = x_0$. Figure 5 shows two such planes; clearly in one case the intersection has one component and in the other case it has two. At the intermediate position, when the plane is tangent to the torus, the intersection will be a curve with a crossing.

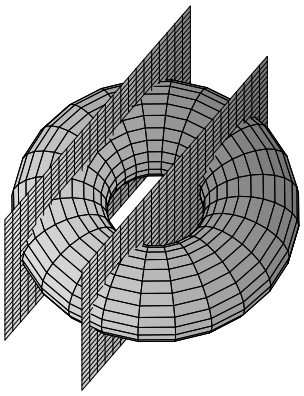

Figure 5: Two planes intersecting a torus.

One problem we have faced when considering such curves is that we have no algorithm for drawing symmetry sets or medial axes of curves given by $f(x, y) = c$. The most straightforward algorithm

available to us, implemented for curves in the package 'Liverpool Surface Modelling Package', is suitable for *parametrized* curves only.

To examine the section $x = x_0$ we therefore proceed as follows. We have $a + b\cos\theta = x_0/\cos\phi$, which gives $\cos\theta = (x_0 - a\cos\phi)/\cos\phi$. We then have

$$y(\phi) = x_0 \tan\phi, \quad z(\phi) = b\sqrt{1 - \left(\frac{x_0 - a\cos\phi}{b\cos\phi}\right)^2},$$

where ϕ ranges over those values for which the right-hand side of the expression for z is real. (Note that in any case we can assume $-\pi/2 < \phi < \pi/2$.) This requires

$$\frac{x_0}{a+b} \leq \cos\phi \leq \frac{x_0}{a-b}. \tag{3}$$

There are two cases:
(i) if $x_0 > a-b$ (the case of a single component to the intersection curve) then the right-hand inequality is vacuous and the left-hand inequality gives say $-\phi_2 \leq \phi \leq \phi_2$ for an acute angle ϕ_2 satisfying $\cos\phi_2 = x_0/(a-b)$. This parametrizes the top half of the intersection curve, and the whole curve can be parametrized by $(Y(\phi),\ Z(\phi))$, where

$$\begin{aligned} Y(\phi) &= \begin{cases} y(\phi) & \text{if } -\phi_2 \leq \phi \leq \phi_2 \\ y(-\phi + 2\phi_2) & \text{if } \phi_2 \leq \phi \leq 3\phi_2 \end{cases} \\ Z(\phi) &= \begin{cases} z(\phi) & \text{if } -\phi_2 \leq \phi \leq \phi_2 \\ -z(-\phi + 2\phi_2) & \text{if } \phi_2 \leq \phi \leq 3\phi_2 \end{cases} \end{aligned}$$

(ii) if $x_0 < a - b$ (the case of two separate intersection curves) then the inequalities (3) give $\phi_1 \leq \phi \leq \phi_2$ or $-\phi_2 \leq \phi \leq -\phi_1$ where $\cos\phi_1 = x_0/(a-b)$ and $\cos\phi_2 = x_0/(a+b)$ and $\phi_1,\ \phi_2$ are acute angles. For each of the two separate intersection curves there are similar formulas to the above for (Y, Z), the ranges of values now being $\phi_1 \leq \phi \leq \phi_2$ and $\phi_2 \leq \phi \leq 2\phi_2 - \phi_1$ for the component of the intersection lying in $y > 0$.

Figures 6 and 7 show respectively examples of (i) and (ii), with the evolute curve also drawn.

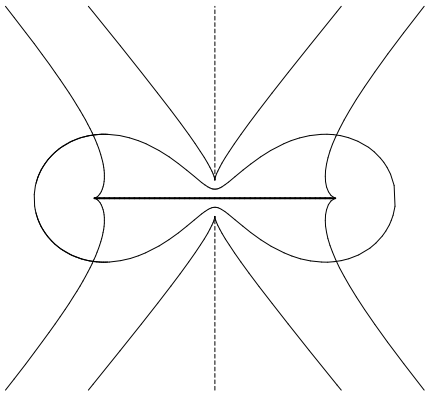

Figure 6: A torus intersection with a single component, close to the singular case $x_0 = a - b$. The evolute is drawn as a thin line, and the medial axis as a thick horizontal line joining the two cusps of the evolute. The vertical dashed line is the remainder of the symmetry set, which also connects cusps of the evolute, via infinity.

From these figures we can deduce the following, which we conjecture are generic phenomena:

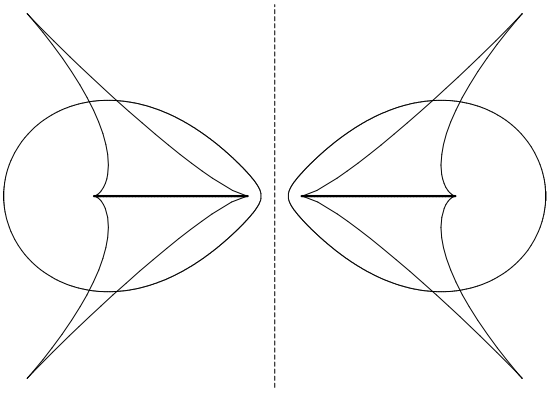

Figure 7: A torus intersection with two components, close to the singular case $x_0 = a - b$. The evolute is drawn as a thin line and the medial axis as two thick horizontal lines. For each component curve, there will be another branch of the symmetry set connecting the other two cusps of the evolute. This branch must pass through the midpoint of the horizontal 'diameter' of the component curve, since there is clearly a bitangent circle enclosing the component whose centre is at this point. There is a further branch of the symmetry set, the vertical dashed line, which corresponds to circles tangent to the *two* components.

1. The medial axis transition through a hyperbolic point is that of one segment splitting to form two (or the reverse, two joining to form one).

2. The symmetry set has additional components, relevant to the structure of the family of curves $f(x, y) = c$ near to the singularity at $c = 0$. A branch (shown dashed in the two figures 6 and 7) exhibits the same behaviour as the medial axis: two segments joining to form one or one splitting to form two. But other segments of the symmetry set can simply appear or disappear in the transition. In the example, there are two vertices on the left-hand component in Figure 7, other than the vertices at the left and right extremities of the component. The presence of these gives the two cusps on the evolute which are not on the axis of symmetry. These two vertices, and that at the right-hand extremity of the component, tend to coincidence as we approach the singular section $x_0 = a - b$. A whole branch of the symmetry set disappears when this happens. We shall investigate this matter in more detail.

Parabolic point at the origin We shall take as an example here the family of curves $x^2 + y^3 = c$, for c close to 0. Figure 8 shows the surface $z = x^2 + y^3$ and planes for two values of c, one negative and one positive. It turns out to be a delicate matter to determine the vertices on these plane sections, in order to obtain information on the branches of the symmetry set. We report here on the beginnings of this work.

Some calculation shows that the vertices of the curve $x^2 + y^3 = c$ occur at $x = 0$ and at values of y for which $g(y, c) = 0$ where

$$g(y, c) = 9y^7 - y^6 - 90cy^4 + 20cy^3 + 8c^2, \text{ and also } y^3 < c,$$

the latter condition ensuring that x is then real. For each y we obtain two values of x, namely $\pm\sqrt{(c - y^3)}$. The question then is: for small values of c, how many solutions of $g(y, c) = 0$ are there close to $y = 0$?

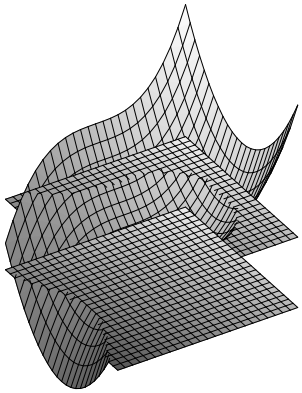

Figure 8: A surface with a parabolic curve and two plane sections near the tangent plane at a parabolic point.

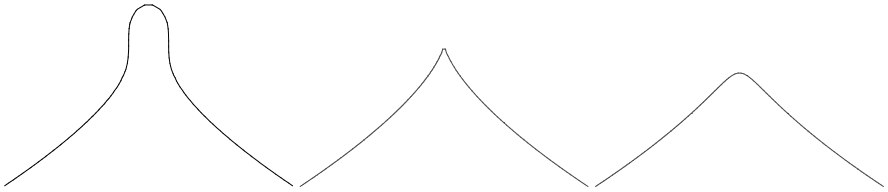

Figure 9: Three sections of the surface above, showing the transition through a cuspidal intersection curve. These curves are of the form $x^2 + y^3 = c$, with $c > 0,\ c = 0,\ c < 0$ from left to right. The x-axis is horizontal and the y-axis vertical, as usual.

The curve $g(y, c) = 0$ is, to lowest order, $c(5y^3 + 2c) = 0$, that is, it has two branches through the origin. These two branches turn out to have series expansions (using Maple) with the coefficients evaluated numerically,

$$c = .049y^3 - .221y^4 - .974y^5 + \ldots, \quad c = -2.549y^3 + 11.471y^4 + .974y^5 + \ldots.$$

Figure 10 shows these two curves, the first one a solid thick line and the second one a dashed thick line, together with the curve $c = y^3$ drawn as a thin line, in the (y, c)-plane with the c-axis vertical. Only points of the two thick curves above the thin curve give real vertices. Thus for small positive and negative c there is one value of y and two vertices on the curve $x^2 + y^3 = c$ besides the one at $x = 0$.

Figure 11 shows the curves $x^2 + y^3 = c$ for a small positive and small negative value of c, together with their evolutes. This shows the two vertices (corresponding to cusps on the evolute).

It appears from this that the medial axis will undergo a transition where its endpoint moves towards the point $(0, c^{1/3})$ on the curve $x^2 + y^3 = c$, coinciding with the cusp on $x^2 + y^3 = 0$ when $c = 0$. The symmetry set on the other hand has two other branches ending at points which approach the curve $x^2 + y^3 = c$ from 'outside'. As $c \to 0$ these branches come closer to the cusp and at $c = 0$ momentarily reach the cusp, before moving away again.

Thus the situation here is quite different from that of the hyperbolic point, where branches of the symmetry set disappear in the transition.

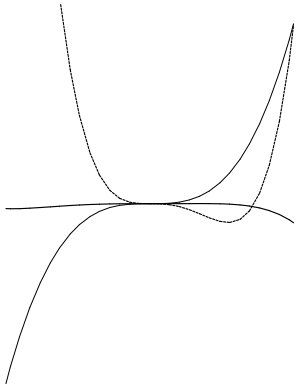

Figure 10: Curves in the (y, c)-plane which determine the positions of vertices on the curve $x^2+y^3 = c$ close to the origin.

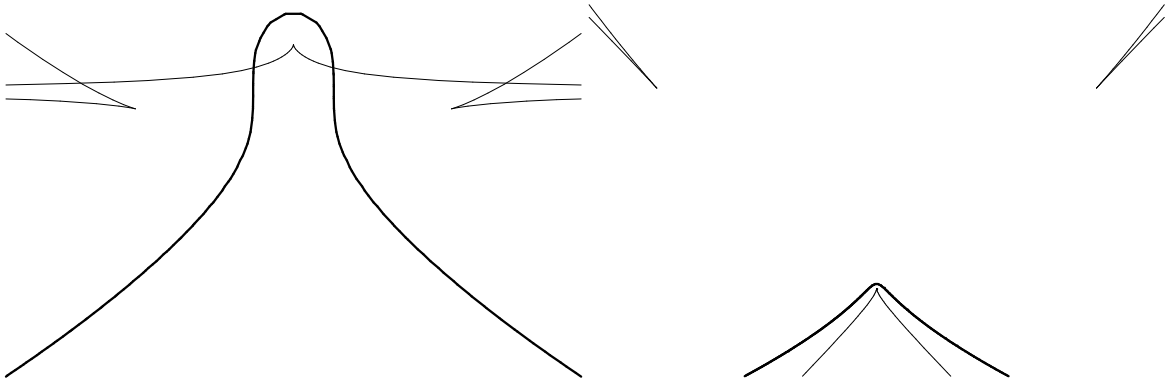

Figure 11: Two of the sections in Figure 9, with their evolutes to show the presence of vertices. The medial axis in each case will go downwards from the cusp on the vertical line of symmetry. There will be branches of the symmetry set coming from infinity and ending in the other cusps of the evolute.

3 Reconstruction from SS or MA

A generic plane curve $\gamma(s)$ can be reconstructed (at least locally) from its SS using a radius function $r(s)$ (radii of tangent circles) defined on its smooth part. To do so, let γ_o stand for the subset of γ consisting of all the (A_1-)ordinary contact points of γ with bitangent circles. If $\gamma(t) \in \gamma_o$, let $u(t)$ be the centre of the corresponding bitangent circle and S_o the collection of all those centres u. In this way, γ_o is the envelope of the circles $C(u(t), r(t))$ centred on $u(t) \in S_o$ with radius $r(t)$. Now if γ is closed, then it is the closure of γ_o.

A reconstruction formula:
We would like to rebuild the local expression of γ_o, say around the origin $(0, 0)$ of S_o, from data on S_o and bitangent circles centred on S_o. As S_o is smooth, the bitangent circles are not osculating at any point of S_o. Let r be the radius of bitangent circles. Using arclengh s as a local parameter on S_o, we suppose $\frac{d}{ds}r(s) \neq 0$ and r does not have a turning point. We can then use r as a parameter on S_o and write $S_o(r)$. Let γ_o^1 and γ_o^2 be the two smooth arcs corresponding to the (local) part of S_o brought in by the circles in both sides of S_o.

The corresponding point in γ_o^i is:

$$x_i = S_o(r) - \frac{r}{|v|}\mathbf{T} - (-1)^i \frac{r}{|v|}\sqrt{v^2 - 1}\mathbf{N}, \;\; i = 1, 2,$$

where **T** and **N** are respectively the unit tangent and the unit normal to S_o (**T,N** is oriented anticlockwise) and $v = \frac{ds}{dr}$.

Now, using the intrinsic reconstruction formula above, one can also derive a relationship between the curvatures of the boundary curve and MA, as follows.

Let us first draw the parallel $\bar{\gamma}_o^i$ to γ_o^i passing through $u(t) \in S_o$, denote $\mathbf{N}_i$ (resp. $\bar{\kappa}_i$) its normal (resp. curvature) at $u(t)$ and ϕ the angle between $\mathbf{T}$ and $\mathbf{N}_1$. Then

$$\kappa = \frac{1}{2}(-\bar{\kappa}_1 + \bar{\kappa}_2) \sin \phi.$$

There are important constraints on the geometry and the dynamics of the medial axis and the symmetry set at special points, namely at the triple crossings on the SS and the corresponding Y junctions on the MA. These arise because from each branch of the SS *two* of the three arcs of the boundary curve can be reconstructed. This means that there are three consistency relations (each involving derivatives of all orders) to be satisfied when all three branches of the SS are taken into account. The simplest consistency relation has the form

$$\sum \frac{\kappa_i}{\sin \phi_i} = 0,$$

where the suffices refer to the three branches of the symmetry set at a triple crossing. The ϕ_i can be interpreted as simply the angles 'opposite' the branches at the crossing. There are many other constraints too; for details see **[12]**.

The same ideas can also be applied in the 3D case; see e.g. **[8]**, **[7]** for some results on this; the consistency relations, which are important in the study of stochastic shape, are studied in the PhD thesis of Pollitt **[14]**.

4 The combinatorics (graph representation) of the MA; its singularities, connectedness etc.

Keeping in mind the idea of looking for the maximum information about the local geometry of SS/MA, we propose here to handle the behaviour of the radius function r, especially near singularities. The SS/MA in 2D can be made an oriented graph if we add arrows and extra vertices corresponding respectively to the flow and the minima/maxima of the radius function r. This provides a refinement of the classification of the SS/MA. Note that in what follows we consider the radius function on the SS as well as the MA. This is important because 'hidden' parts of the SS do contribute to the evolution of the MA, as is made evident by Figures 3,4. Thus we have looked specifically at the radius function at the different singularities as in Section 1.2 and at the changes that occur in the radius function at the transitions of the SS which were listed in Section 2.

• A_1A_2: The behaviour of the flow of r at a cusp corresponding to an A_1A_2, was not described so far in the literature. Hence, we present here some details of our calculations. Assume γ is unit speed. Consider the two branches $\gamma_1(t)$ and $\gamma_2(s)$ of γ corresponding respectively to the A_1 and A_2 contact points with the circle, where s and t are local variables. Set $N_1(t)$, $N_2(s)$ the respective normals to γ at $\gamma_1(t)$ and $\gamma_2(s)$, and r the radius of the circle. Note that in the A_1A_2 case, using the implicit function theorem, one expresses t as a local smooth function $t = t(s)$ of s.
The centre of this circle being $\gamma_1(t) + rN_1(t)$ or equivalently $\gamma_2(s) + rN_2(s)$, we can then write

$$\gamma_1(t) - \gamma_2(s) = r(s)(N_2(s) - N_1(t)). \tag{4}$$

Differentiating the above expression **(4)** with respect to s, we have

$$t'(s)T_1(t) - T_2(s) = r'(N_2(s) - N_1(t)) + r(-\kappa_2(s)T_2(s) + t'(s)\kappa_1(t)T_1(t)). \tag{5}$$

or equivalently

$$t'(s)(1 - r\kappa_1(t))T_1(t) = r'(N_2(s) - N_1(t)) + (1 - r\kappa_2(s))T_2(s). \tag{6}$$

Up to a reparametrization, we can always assume that $s = 0$ corresponds to the A_2 contact point with the circle and that $t = 0$ when $s = 0$.

At this step, let's take into account the two following facts. In one hand, the circle is a circle of curvature at the A_2 contact point, that is $\kappa_2 = \frac{1}{r}$. So that, at $s = 0$, the equation **(6)** becomes $t'(1 - r\kappa_1)T_1 = r'(N_2 - N_1)$. The dot product with N_1 gives

$$r'(0)(N_2.N_1 - 1) = 0.$$

From the chosen orientation, we cannot have $N_1.N_2 = 1$ and we can rewrite the above equation as follows

$$r'(0) = 0 \text{ and } t'(0)(1 - r\kappa_1)T_1 = 0. \tag{7}$$

In the other hand, the dot product of T_1 and this latter gives the following equation $t'(0)(1-r\kappa_1) = 0$. But since the A_1 is an ordinary point contact $r\kappa_1$ should be different from 1. It follows that $s = 0$ is a singularity of $t(s)$, that is $t'(0) = 0$ and consequently the A_1 point contact is a turning point in the parameter (s, t)-space. Hence we are finally left with

$$r'(0) = 0 \text{ and } t'(0) = 0. \tag{8}$$

To handle the behaviour of r, we need the sign of its second derivative, which we get from **(5)**.

$$\begin{aligned} t''T_1 + (t')^2\kappa_1 N_1 - \kappa_2 N_2 = \quad & r''(N_2 - N_1) + 2r'(-\kappa_2 T_2 + t'\kappa_1 T_1) \\ & + r(-\kappa_2' T_2 - \kappa_2^2 N_2 + t''\kappa_1 T_1 + (t')^2(\kappa_1' T_1 + \kappa_1^2 N_1)). \end{aligned}$$

Now at $s = 0$, using again $t'(0) = 0$, $r = \frac{1}{\kappa_2}$, and $r'(0) = 0$, the above equation reads

$$t''T_1 = r''(N_2 - N_1) - \frac{\kappa_2'}{\kappa_2}T_2 + t''\frac{\kappa_1}{\kappa_2}T_1.$$

Again, the dot product with N_1, leads to the following.

$$r''(N_2.N_1 - 1) = \frac{\kappa_2'}{\kappa_2}T_2.N_1 \tag{9}$$

Notice that we are not at an A_1A_3 singularity of the distance squared function, this means in particular $\kappa_2' \neq 0$.

- If the A_1 and A_2 points contact with the circle, are not diametrically opposed, we also have $T_2.N_1 \neq 0$. That is, $r''(0) \neq 0$ and r has an extremum at $s = 0$. Such an extremum is a minimum if and only if γ_1 is on the same side of the normal at $\gamma_2(0)$ as the part of γ_2 inside the circle.

- Now in the special case where the A_1 and A_2 points contact are diametrically opposed, we have $T_2.N_1 = 0$ and r has a degenerate singularity (inflexion) $r' = r'' = 0$. Such an inflexion of r appears on the SS during an evolution, say through a 1-parameter family of curves. See Figure 12.

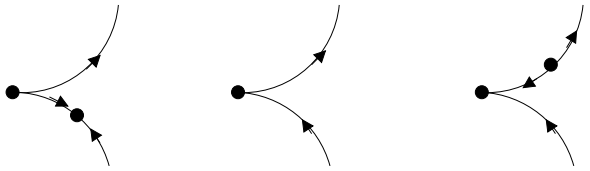

Figure 12: A turning point of r moving through a cusp on the symmetry set: this happens when there is an A_1A_2 point where the tangents to the boundary curve are parallel. The turning points of r are marked with dots: two turning points come together to make an inflexion (degenerate turning point) of r. This occurs when the contact points of the corresponding circle are diametrically opposite.

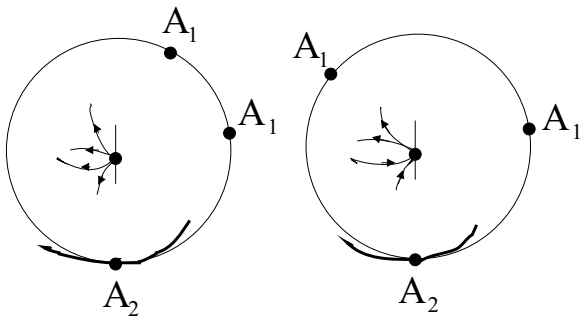

Figure 13: Schematic drawing of the radius at an $A_1^2A_2$ transition. Here we assume that the curve enters the circle to the right of the A_2 point, as sketched.

• $A_1^2A_2$: This case similar to the A_1A_2 and almost the same scenarios happen (Figure 13). Indeed applying the same calculation as above, we get two cases here. If the two A_1 points contact are on the same side at the A_2 point contact as the part of γ_2 (containing the A_2) inside the cercle, then r has only minima at the two cusps. Otherwise, there is one minimum and one maximum of r.
In the rest of the cases, the flow of r essentially follows from a compatibility condition on the local geometry of SS/MA. Here is the list with few comments.

• A_2^2: – The nib case. As two cusps of the SS interact and exchange branches, each of the different branches brings the behaviour of r on it. So that, the flow of r must be consistant with either sides: before and after the transition.

That is, during transitions through an A_2^2 'nib' singularity, the radius has to be always simultaneously increasing (resp. simultaneously decreasing) in both branches as indicated in Figure 14

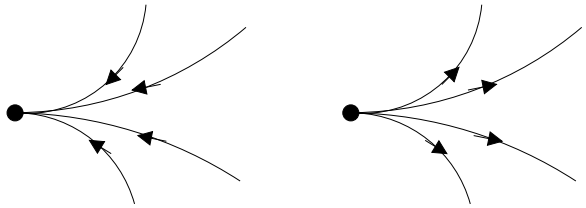

Figure 14: The radius function at a nib transition has maxima on both cusped branches (left) or minima on both (right).

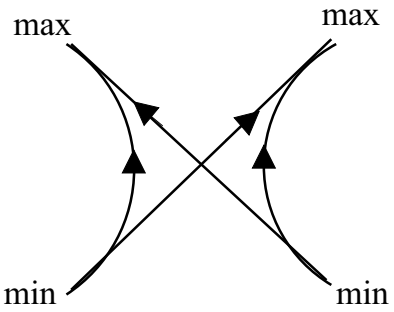

Figure 15: The radius function at a moth transition has two maxima and two minima.

– The moth case. The only way that is geometrically allowed for the behaviour of r is, each cusp being an extremum of r. Hence there will be two maxima and two minima of r, as shown in Figure 15

• A_1A_3: Here, using the condition that, in the MA, two arrows must come into the (triple in the MA) crossing point, we have the following scenaerio (see Figure 15).

• A_4 The only geometrically allowed way of behaviour for the flow of r, is obviously r increasing from a minimum towards a maximum at a vertex, then decreasing to a minimum on the other vertex and again increasing.

• A_1^3: Now we have a tripple crossing point. There are two cases depending on whether all those three A_1-contact points are in the same semi-circle including the case where two points diametrically opposed, or none of those first two cases.

– In the first case, we there are two arrows coming into the crossing point (r increasing towards that crossing point) and one arrow going out (r increasing away from the triple crossing point).

– In the second case, we have three arrows coming into the crossing point, ie r is increasing in all branches towards a maximum at the crossing point.

• A_1^4: We also have the same scenarios as above, with all the arrows coming into the crossing point if the four A_1 contact points are not all in the same semi-circle including the case where two points diametrically opposed. Otherwise, there is only one arrow going out from the crossing point.

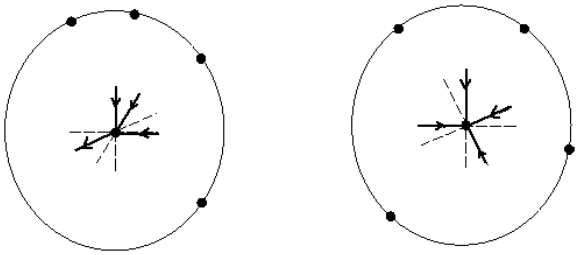

Figure 16: Radius at ss-A_1^4 transition.

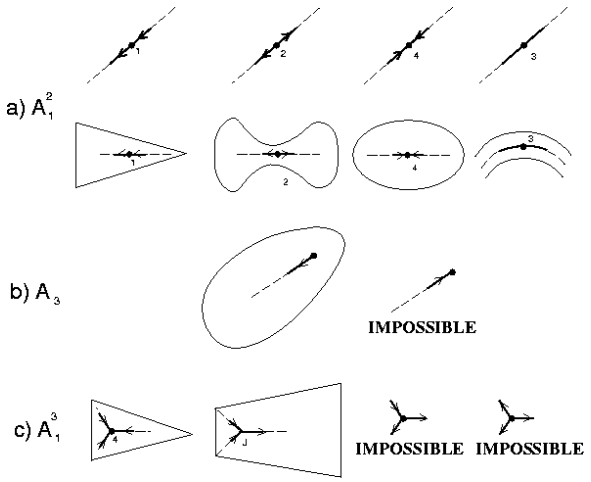

Figure 17: Radius on the SS A_1^2, A_1^3 and A_3-points.

5 Conclusion

We have examined the symmetry set and medial axis in 2D, giving known results on the structure for a single curve and in a 1-parameter family of curves, and also in a 1-parameter family evolving by mean curvature motion.

We have indicated the beginnings of a new investigation into the case of a family of sections of a generic surface—this is very different from the case of a generic family of smooth curves since singularities (crossings, cusps, etc.) may arise in the curves whose symmetry sets we are considering. We are used to singularities of the SS or MA but not to singularities of the curve whose SS/MA we are constructing. It is not clear at this stage which results of singularity theory will give general theorems here.

We have also considered the radial flow in 2D, giving some new results on the radial flow on the SS, including results on families of curves. As yet we do not have results on matching trees and seek input from other members of the research group.

The 3D cases of all these investigations will be more technically demanding than the 2D cases. We already know about the evolution of the MA in 3D (work of Bogaevsky) and we have begun the evolution of the SS in 3D. This work is for the future.

References

[1] Bogaevsky, I. A., *Perestroikas of shocks and singularities of minimum functions.* Physica D: Non Linear Phenomena, DEC/2002, vol 173/1-2 pp. 1-29.

[2] Bruce, J.W., 'Functions on discriminants', *J.London Math. Soc* 30 (1984), 551–567.

[3] Bruce, J. W.; Giblin, P. J. 'Growth, motion and 1-parameter families of symmetry sets', *Proc. Roy. Soc. Edinburgh Sect. A* 104 (1986), no. 3-4, 179-204.

[4] Bruce, J. W.; Giblin, P. J. *Curves and singularities. A geometrical introduction to singularity theory.* Cambridge University Press, Cambridge, 1984, Second Edition 1992.

[5] Bruce, J. W.; Giblin, P. J.; Gibson, C. G. ‘Symmetry sets’, *Proc. Roy. Soc. Edinburgh Sect. A* 101 (1985), no. 1-2, 163-186.

[6] J.W.Bruce, P.J.Giblin and F.Tari, ‘Parabolic curves of evolving surfaces,’ *Int. J. Computer Vision.* 17 (1996), 291–306.

[7] Damon, J. *Determining the geometry of boundaries of objects from medial data* (to appear)

[8] Giblin, P.J. ‘Symmetry sets and medial axes in two and three dimensions’, *The mathematics of surfaces, IX* (Cambridge, 2000), 306-321, Springer, London, 2000.

[9] Giblin, P. J.; Brassett, S. A. ‘Local symmetry of plane curves’, *Amer. Math. Monthly* 92 (1985), no. 10, 689-707.

[10] Gage, M.; Hamilton, R.S. *The heat equation shrinking convex plane curves.*J. Diff. Geom. 23 (1986), no. 1, 69-96.

[11] Giblin, P.J.; Kimia, B. ‘On the Local Form and Transitions of Symmetry Sets, and Medial Axes, and Shocks in 2D’, *Proceedings of the Fifth International Conference on Computer Vision (ICCV99)* IEEE Computer Society Press (1999), 385–391.

[12] P.J.Giblin and B.B.Kimia, ‘On the Intrinsic Reconstruction of Shape from its Symmetries’, to appear in IEEE Trans. Pattern Recognition and Image Analysis.

[13] Giblin, P.J.; Kimia, B. ‘A formal classification of 3D medial axis points and their geometry’, to appear in *Pattern Analysis and Machine Intelligence*, 2003.

[14] Pollitt, A.J., *Euclidean and Affine Symmetry Sets and Medial Axes*, Ph.D. thesis, University of Liverpool. In preparation.

[15] Teixeira R. C. ‘Medial axes and Mean Curvature Motion II: Singularities’, (to appear.)